PROCEEDINGS OF SCIENCE

Measurement of the ridge correlations in pp and p+Pb collisions with the ATLAS detector at the LHC

Klaudia Burka* **on behalf of the ATLAS Collaboration**
Institute of Nuclear Physics Polish Academy of Sciences,
ul. Radzikowskiego 152, 31-342 Cracow, Poland
E-mail: kburka@cern.ch

The ATLAS measurement of azimuthal correlations between particle pairs at large pseudorapidity separation in pp and p+Pb collisions are presented. The data were collected using a combination of the minimum-bias and high track-multiplicity triggers. A detailed study of the dependence of two-particle correlations on the charged particle multiplicity, transverse momentum of the pair constituents and the pseudorapidity separation between particles forming a pair is shown. The transverse momentum dependence of a single particle azimuthal anisotropy coefficients, $v_2 - v_5$ in p+Pb and v_2 in pp collisions are also presented. These measurements of the long-range correlations in high-multiplicity pp and p+Pb collisions provide insight into flow phenomena in heavy ion collisions.

XXIV International Workshop on Deep-Inelastic Scattering and Related Subjects
11-15 April, 2016
DESY Hamburg, Germany

*Speaker.

PoS(DIS2016)053

1. Introduction

The main goal of ultra-relativistic heavy ion physics is to study the Quark-Gluon Plasma (QGP), produced in nuclear collisions at the Relativistic Heavy Ion Collider (RHIC) and the Large Hadron Collider (LHC) e.g. in ATLAS experiment [1]. QGP is a very dense and hot system, formed of unbound quarks and gluons, lasting for a fraction of a second after the collision. Due to large pressure gradients inside the QGP region, originating from an asymmetry in the initial geometry of the interacting nucleons, produced particles are emitted in preferential directions. Hence, one of the signatures of QGP is azimuthal anisotropy of single particle distribution, which represents a response of the medium to the initial state condition. Experimetntally, the initial conditions of QGP dynamics are studied using particle correlations in the final stage, commonly expressed via Fourier series of the azimuthal distributions with coefficients known as flow harmonics [2]. The second flow harmonic, so-called *elliptic flow*, is related to the initial elliptical shape of the collision zone. Higher harmonics correspond to spatial fluctuations of the interaction region. The QGP is a high-density system where many partons are compressed in a small volume. Studying the multi-particle correlations originating from such systems is essential for understanding their properties. Customarily, the two particle correlation (2PC) function in relative pseudorapidity, $\Delta\eta = \eta_a - \eta_b$ and relative azimuthal angle, $\Delta\phi = \phi_a - \phi_b$ is used in such analyses. Recent studies of 2PC in high-multiplicity pp, p+A and A+A collisions show distinct long-range correlations in $\Delta\eta$ at $\Delta\phi \approx 0$ (near-side peak) and $\Delta\phi \approx \pi$ (away-side peak). The long-range structure, commonly called the "ridge", was first discovered in heavy-ion collisions at RHIC [3–5] and then studied in great detail at the LHC [6–8]. The ridge is interpreted as a simple manifestation of the single particle azimuthal anisotropies, which originate from the collective expansion of the QGP medium. Latest results show that "ridge" structures are also observed in high-multiplicity pp [9, 10] and p+Pb [11–14] colliding systems. These observations are remarkable as it was generally believed that the long range correlation would not be seen in small colliding systems, where collective expansion was not likely to develop. The underlying mechanism of the ridge in pp and p+Pb collisions is not yet fully understood. However, recent reports suggested that it might originate from collective sinusoidal $(\cos(2\phi))$ modulation of the single particle distributions with the amplitude given by the second Fourier harmonic v_2. This paper summarizes the recent ATLAS results on long-range correlation measurements in p+Pb and pp collisions.

2. Event and track selections

The results presented in this report are based on 14 nb^{-1} of $\sqrt{s} = 13$ TeV pp data recorded during the LHC run in 2015 [10]. For comparison, measurements for two sets of 1 μb^{-1} and 28 nb^{-1} $\sqrt{s_{\rm NN}} = 5.02$ TeV p+Pb data recorded in 2012 and 2013, respectively, were also used [13,14]. Both, pp and p+Pb, measurements were performed using the data reconstructed by ATLAS Inner Detector [1] with tracking coverage of $|\eta| < 2.5$ and $p_{\rm T} > 0.4$ GeV. Furthermore, in the p+Pb system, the Forward Calorimeter (FCal) [1] was used to define the event activity. Both measurements benefit from the dedicated high-multiplicity triggers (HMT) combined with minimum-bias triggers in order to enhance the sample with high-multiplicity events. In pp collisions, the 2PC functions are measured in multiplicity, $N_{\rm ch}^{\rm rec}$, intervals, whereas in p+Pb collisions measurements are done in different event activity classes. The event activity can be characterized either by the total transverse energy, $\sum E_{\rm T}^{\rm Pb}$, measured by the FCal over $-4.9 < \eta < -3.2$ at the Pb - fragmentation side or the

charged track multiplicity, $N_{\mathrm{ch}}^{\mathrm{rec}}$, similarly to the pp case. Nuclear collisions with high event activity (high $\sum E_{\mathrm{T}}^{\mathrm{Pb}}$ or high $N_{\mathrm{ch}}^{\mathrm{rec}}$) have on average a larger number of participating nucleons and a small impact parameter. Therefore, terms *central* and *peripheral* can be also used to describe high and low event activity - similarly to the approach adopted in Pb+Pb collisions.

3. The ridge measurement in p+Pb and pp collisions

The two particle correlation in azimuthal relative angle and relative pseudorapidity is constructed from the ratio of the distributions of the number of pairs in the same-event (signal) and mixed-event (background) [13, 14]:

$$C(\Delta\phi,\Delta\eta) = \frac{S(\Delta\phi,\Delta\eta)}{B(\Delta\phi,\Delta\eta)}. \tag{3.1}$$

The mixed-event part, $B(\Delta\phi,\Delta\eta)$, is constructed from pairs of particles taken from different events with similar centrality and z - component of the vertex. The mixed-event technique is designed to remove residual structures due to the detector acceptance. The two particles involved in the correlation are typically selected with different conditions: different transverse momentum, p_{T}, pseudorapidity ranges, different charge sign or species. In the analysis the particles are denoted as particle 'a' and particle 'b' corresponding to the *trigger* and *reference* particle, respectively.

3.1 2PC in p+Pb collisions

Panels (a) and (b) in Fig.1 show examples of 2PC functions extracted from peripheral and central p+Pb collisions, respectively. Both trigger and reference particles were selected from $0.5 < p_{\mathrm{T}}^{\mathrm{a,b}} < 4$ GeV range. The correlation function for peripheral events shows a sharp peak cen-

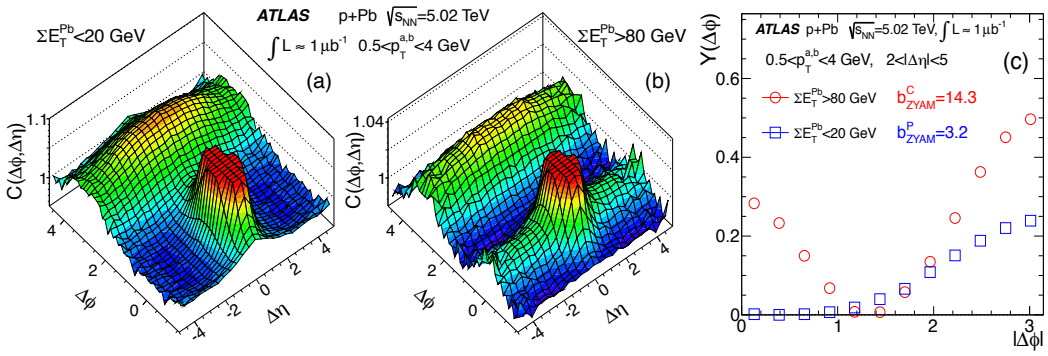

Figure 1: The two-particle correlation functions for peripheral (a) and central (b) events. The peak at $(\Delta\phi,\Delta\eta)$ = (0,0) is truncated to better show the long range correlations. (c) The distribution of per-trigger yields for pairs integrated over $0.5 < p_{\mathrm{T}}^{\mathrm{a,b}} < 4$ GeV and $2 < |\Delta\eta| < 5$ for central (red points) and peripheral (blue squares) events [13].

tered at $(\Delta\phi,\Delta\eta)$ = (0,0). This peak results from pairs that originate from the same jet, Bose-Einstein correlations or high-p_{T} resonance decays. Furthermore, there is a broad structure at $\Delta\phi \approx \pi$ which is interpreted as contributions from dijets (recoil) or low-p_{T} resonances. The 2PC function for central events presents the same structures from jets and dijets around $\Delta\phi \approx 0$ and π but in contrast to peripheral events, it reveals a clearly visible ridge-like structure at the near-side

($\Delta\phi \approx 0$) along $\Delta\eta$. In order to investigate properties of the ridge-like structures, the $\Delta\eta$ is limited to long range region of $2 < |\Delta\eta| < 5$. The strength of the long-range correlations is estimated by using per-trigger particle yield, which measures the average number of particles correlated with each trigger particle. The per-trigger yield, $Y(\Delta\phi)$, is a one-dimensional (1D) function of $\Delta\phi$ [13]:

$$Y(\Delta\phi) = \left(\frac{\int B(\Delta\phi) d\Delta\phi}{\pi N_a} \right) C(\Delta\phi) - b_{\mathrm{ZYAM}}, \tag{3.2}$$

where $C(\Delta\phi)$ function is obtained by dividing the numerator and denominator in Eq. 3.1 but integrated earlier over $2 < |\Delta\eta| < 5$. The N_a corresponds to the number of trigger particles and the b_{ZYAM} parameter is a constant correcting the per-trigger yield for contribution from uncorrelated pairs. The b_{ZYAM} is evaluated using the zero-yield-at-minimum (ZYAM) method [15, 16]. Panel (c) in Fig. 1 shows the distributions of per-trigger yields in central and peripheral events integrated over $2 < |\eta| < 5$, after subtracting the b_{ZYAM} pedestal ($\Delta\phi$ is folded to $0 < |\Delta\phi| < \pi$). The yield in central events shows the near-side and away-side peaks with modulation similar to $\cos(2\Delta\phi)$, while in the peripheral yield there is only an away-side peak. The difference between central and peripheral yields shows a constant excess in the near- and away-side peaks. This suggests that peripheral events contain mainly the short-range correlation component and away-side peak. Thus, to better quantify ridge structures, the distribution for peripheral events is subtracted from the one for more central events. Finally, the subtracted per-trigger yield, Y^{sub} is expressed via a Fourier series, similar to the approach used in Pb+Pb collisions [14]:

$$Y^{sub}(\Delta\phi) = Y(\Delta\phi) - \alpha Y_{\mathrm{periph}}(\Delta\phi) \propto \left[1 + \sum_n 2 v_{n,n} cos(n\Delta\phi) \right]. \tag{3.3}$$

The $v_{n,n}$ coefficients correspond to long-range correlations in two-particle Fourier distribution.

3.2 2PC in *pp* collisions

The 2PC function in *pp* collisions has similar structures as it is seen for *p*+Pb collisions. Panels (a) and (b) in Fig.2 show the example correlation functions for *pp* collisions at $\sqrt{s} = 13$ TeV for pairs integrated over $0.5 < p_{\mathrm{T}} < 5$ GeV in low- and high-multiplicity events of $10 < N_{\mathrm{ch}}^{\mathrm{rec}} < 30$

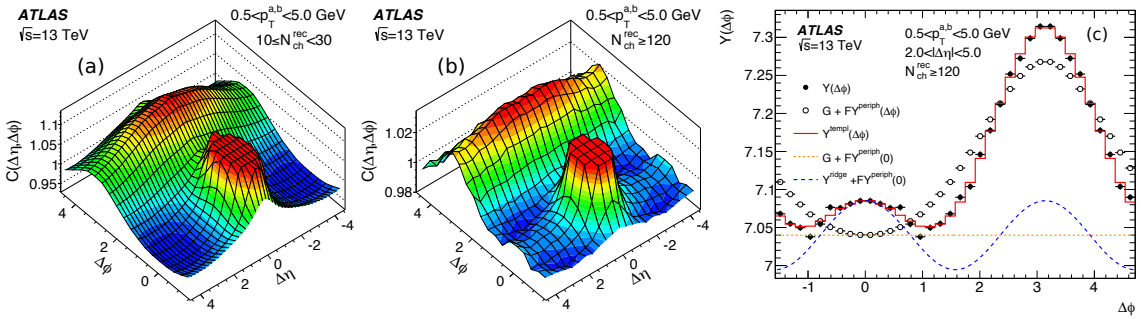

Figure 2: The two-dimensional correlation functions in *pp* collisions integrated over $0.5 < p_{\mathrm{T}}^{\mathrm{a,b}} < 5$ GeV shown for low- (a) and high-multiplicity (b) events. (c) The per-trigger particle yield for high-multiplicity events, $N_{\mathrm{ch}}^{\mathrm{rec}} > 120$, with the template fit example [10].

and $N_{\mathrm{ch}}^{\mathrm{rec}} > 120$, respectively. The characteristic long-range structures are clearly seen in *pp* high-multiplicity events. The procedure to quantify ridge is different in the case of *pp* collisions than

previously described. The ZYAM method is no longer accurate as the ZYAM pedestal is distorted to the contributions of the long-range correlations or away-side peak dominated by dijets. As a result, the b_{ZYAM} parameter might be over- or underestimated. Therefore, a new template fitting method was developed and applied in pp measurements. In this approach, the measured $\mathrm{Y}(\Delta\phi)$ distributions are assumed to result from a superposition of a low-multiplicity $\mathrm{Y}^{\mathrm{periph}}$ distribution, scaled up by a multiplicative factor, F, and an elliptic modulation $\cos(2\Delta\phi)$ [14]:

$$Y^{\mathrm{templ}}(\Delta\phi) = FY^{\mathrm{periph}}(\Delta\phi) + Y^{\mathrm{ridge}}(\Delta\phi), \;\; Y^{\mathrm{ridge}}(\Delta\phi) \approx (1 + 2v_{2,2}cos(2\Delta\phi)) \tag{3.4}$$

Panel (c) in Fig.2 shows an example of template fitting results. The plot is made for high-multiplicity events in long-range region $|\Delta\eta| > 2$ integrated over $0.5 < p_{\mathrm{T}}^{\mathrm{a,b}} < 5$ GeV. The scaled $\mathrm{Y}^{\mathrm{periph}}$ distribution is shown with open points. The $\mathrm{Y}^{\mathrm{ridge}}$ is shown with a dashed blue line and the full template fit function is marked with the red solid line. The resulting template fit is in good agreement with the data denoted by black points. The $\mathrm{Y}^{\mathrm{ridge}}$ is proportional to Fourier component with the amplitude $v_{2,2}$ similarly to that in p+Pb colliding system.

4. Results

Both p+Pb and pp per-trigger yields can be expressed by the Fourier cosine component with the amplitude of $v_{2,2}$. The $v_{2,2}$ corresponds to the Fourier coefficient in the two particle azimuthal distribution. If the cosine of $2\Delta\phi$, for pp and p+Pb, arises from the modulation of the single particle distributions then $v_{2,2}$ should factorize as: $v_{2,2}(p_{\mathrm{T}}^{\mathrm{a}}, p_{\mathrm{T}}^{\mathrm{b}}) = v_2(p_{\mathrm{T}}^{\mathrm{a}})v_2(p_{\mathrm{T}}^{\mathrm{b}})$, where $v_{2,2}$ depends on both particles transverse momentum while v_2 depends only on trigger or reference particle p_{T}. Then $\mathrm{v}_2(p_{\mathrm{T}}^{\mathrm{a}}) = v_{2,2}(p_{\mathrm{T}}^{\mathrm{a}}, p_{\mathrm{T}}^{\mathrm{b}})/\sqrt{v_{2,2}(p_{\mathrm{T}}^{\mathrm{b}}, p_{\mathrm{T}}^{\mathrm{b}})}$. It was shown that such factorization works fine for both colliding systems [10, 14]. This suggests that long-range correlation structures observed in

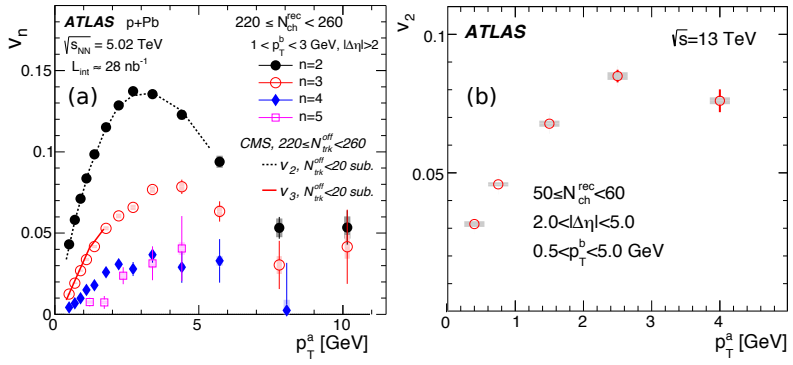

Figure 3: (a) The $v_n(p_{\mathrm{T}}^{\mathrm{a}})$ harmonics for n=2-5 measured in high-multiplicity p+Pb collisions [14]. (b) The $v_2(p_{\mathrm{T}}^{\mathrm{a}})$ measured in one multiplicity interval in pp collisions [10].

pp and p+Pb systems might originate from the same single particle global azimuthal anisotropy as in Pb+Pb collisions. Panel (a) in Fig.3 presents harmonics $v_2 - v_5$ as a function of $p_{\mathrm{T}}^{\mathrm{a}}$ in high-activity bin. For a comparison, the CMS results for v_2 and v_3 in a similar activity bin are also plotted (dashed lines) [17]. Panel (b) shows the $v_2(p_{\mathrm{T}}^{\mathrm{a}})$ results for pp collisions at 13 TeV in one multiplicity bin, integrated over long-range correlation region and $p_{\mathrm{T}}^{\mathrm{b}}$ = 0.5 - 5 GeV. The $\mathrm{v}_2(p_{\mathrm{T}}^{\mathrm{a}})$ in both collision systems shows similar tendency: it rises with $p_{\mathrm{T}}^{\mathrm{a}}$ up to around 3 GeV and then falls for higher $p_{\mathrm{T}}^{\mathrm{a}}$. Such behavior is also observed in Pb+Pb collisions, where it originates from single particle azimuthal anisotropy [8].

The centrality dependence of v_2 for p+Pb collisions for particle pairs with $0.4 < p_{\mathrm{T}}^{a,b} < 3$ GeV is shown in panel (a) in Fig.4. Panel (b) in Fig.4 presents the v_2 dependence on multiplicity for

pairs with $0.5 < p_{\mathrm{T}}^{a,b} < 5$ GeV in pp collisions. In p+Pb system, integrated elliptic flow increases significantly with the event-activity and at high $N_{\mathrm{ch}}^{\mathrm{rec}}$ it saturates, whereas v_2 in pp system shows no multiplicity dependence.

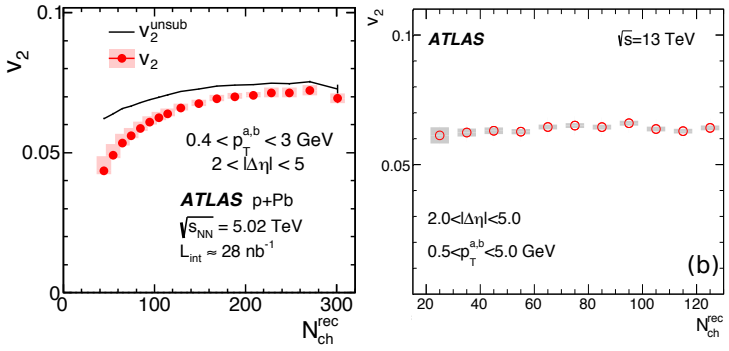

Figure 4: (a) The $v_2(N_{\mathrm{ch}}^{\mathrm{rec}})$ distribution for pairs with $0.4 < p_{\mathrm{T}}^{a,b} < 3$ GeV in p+Pb collisions. The results are presented for v_2 with (points) and without (line) peripheral subtraction [14]. (b) The multiplicity dependence of v_2 measured for pairs with $0.5 < p_{\mathrm{T}}^{a,b} < 5$ GeV in pp collisions [10].

5. Summary

The high-precision measurements of the azimuthal anisotropy were performed in pp and p+Pb collisions by ATLAS. The ridge structures were observed in high-multiplicity 13 TeV pp collisions as well as in 5.02 TeV p+Pb collisions. The ZYAM and template fitting methods were applied to extract long range modulation of the correlation functions $\langle\cos(2\Delta\phi)\rangle$. The amplitudes of these modulation, $v_{2,2}$, exhibit factorization into single particle v_2. Therefore, the p_{T} dependence of v_2 was measured for both systems. For p+Pb collisions the higher harmonics were also measured. The dependence of v_2 on p_{T} in pp and p+Pb is similar to that observed in Pb+Pb collisions. This suggests that the ridge in pp, p+Pb and Pb+Pb collisions might arise from a similar dynamics.

This work was supported in part by the National Science Centre, Poland grant 2015/18/MST2/00087 and by PL-Grid Infrastructure.

References

[1] ATLAS Collaboration, JINST **3** (2008) S08003.
[2] A. M. Poskanzer and S. A. Voloshin, Phys. Rev. **C58** (1998) 1671–1678.
[3] A. Adare et al., PHENIX Collaboration, Phys. Rev. C **78** (2008) 014901.
[4] B. I. Abelev et al., STAR Collaboration, Phys. Rev. C **80** (2009) 064912.
[5] B. Alver et al., PHOBOS Collaboration, Phys. Rev. Lett. **104** (2010) 062301.
[6] K. Aamodt et al., ALICE Collaboration, Phys. Lett. **B708** (2012) 249–264.
[7] CMS Collaboration, Eur. Phys. J. **C72** (2012) 2012.
[8] ATLAS Collaboration, Phys. Rev. **C86** (2012) 014907.
[9] CMS Collaboration, JHEP **09** (2010) 091.
[10] ATLAS Collaboration, Phys. Rev. Lett. **116** no.~17, (2016) 172301, https://atlas.web.cern.ch/Atlas/GROUPS/PHYSICS/PAPERS/HION-2015-09/.
[11] CMS Collaboration, Physics Letters B **718** (2013) 795 – 814.
[12] B. Abelev et al., ALICE Collaboration, Phys. Lett. **B719** (2013) 29–41.
[13] ATLAS Collaboration, Phys. Rev. Lett. **110** no.~18, (2013) 182302.
[14] ATLAS Collaboration, Phys. Rev. **C90** no.~4, (2014) 044906, https://atlas.web.cern.ch/Atlas/GROUPS/PHYSICS/PAPERS/HION-2013-04/.
[15] N. N. Ajitanand et al., Phys. Rev. **C72** (2005) 011902.
[16] A. Adare et al., PHENIX Collaboration, Phys. Rev. **C78** (2008) 014901.
[17] CMS Collaboration, Physics Letters B **724** (2013) 213 – 240.